except those bonding to C(1) were refined isotropically. The fractional atomic parameters and the interatomic bond distances and angles are given in the Supplementary Material.

Acknowledgment. We are grateful to Dr. Y. Takai of The Institute of Scientific and Industrial Research, Osaka University for measuring the ^1H NMR spectra and for valuable discussions.

Supplementary Material Available: Listing of the bond distances, bond angles, fractional atomic coordinates, and anisotropic thermal parameters for non-hydrogen atoms (3 pages). Ordering information is given on any current masthead page.

Structure of Brevetoxin A as Constructed from NMR and MS Data

Jan Pawlak,[†] Michael S. Tempesta,[†⊥] Jerzy Golik,[†] Michael G. Zagorski,[†] Min S. Lee,[†] Koji Nakanishi,*[†] Takashi Iwashita,[‡] Michael L. Gross,[§] and Kenneth B. Tomer[§]

Contribution from the Department of Chemistry, Columbia University, New York, New York 10027, Suntory Institute for Bioorganic Research, Shimamoto-cho, Mishima-gun, Osaka 618, Japan, and Midwest Center for Mass Spectrometry, University of Nebraska, Lincoln, Nebraska 68858-0362. *Received August 18, 1986*

Abstract: Brevetoxins (BTX) exemplified by BTX-B $C_{50}H_{70}O_{14}$ (**1**) are neurotoxins produced by *Gymnodinium breve*. The blooms of these dinoflagellates known as red tide have led to massive fish kills, mollusk poisoning, etc. along the Florida coast and the Gulf of Mexico. Up to date, a total of five BTX's with the same skeleton have been found. The skeleton is an unprecedented array of trans-linked 6/6/6/7/7/6/6/8/6/6/6-membered rings, one δ-lactone and ten ether rings, leading to a stiff ladderlike linear structure. The structure of BTX-A $C_{49}H_{70}O_{13}$ (2), recently determined by X-ray crystallography, has an even more unique oxacarbocyclic skeleton made up of 5/8/6/7/9/8/8/6/6/6-membered rings. An independent study based solely on spectroscopic data, namely NMR and MS has led to the same structure except for an error in the configuration of one methyl group (at C-6). It was possible to construct the entire skeleton of BTX-A from the NMR data and MS of two derivatives. Two general fragmentation patterns in the MS of brevetoxin derivatives were recognized, and it was these patterns, assisted by NMR data, which enabled one to reconstruct the structure of brevetoxin A in a logical manner.

The red tide dinoflagellate *Gymnodinium breve* (*Ptychodiscus brevis* Davis) is responsible for massive fish kills and food poisoning occurring in the Gulf of Mexico and along the coast of Florida.[1] The brevetoxins, the causative agents of the poisoning, have attracted considerable interest since 1968;[2] they are lipid soluble neurotoxins which block the neuromuscular action.[3]

The full structure of the first member of these toxins, brevetoxin B ($C_{50}H_{70}O_{14}$) (BTX-B) (1), elucidated in 1981,[4] was of unprecedented nature. Namely, it consists of 11 oxygen-containing trans fused 6/6/6/7/7/6/6/8/6/6/6 rings condensed in a ladder shape, 30 Å long, 6 Å wide, and 6 Å high, the only flexible portion in the polyether skeleton being the site of the two seven-membered rings. The structures of five more toxins in this series have since been elucidated, i.e., BTX-C,[5] GB-3,[6] GB-5,[7] and GB-6.[7,8] Recently[9] the structure of a new member of the brevetoxins BTX-A (GB-1 toxin) ($C_{49}H_{70}O_{13}$), which had remained unknown because of its poor crystallinity, was finally elucidated by X-ray crystallography as **2**, another extraordinary structure consisting of trans fused 5/8/6/7/9/8/8/6/6/6 lactone-ether rings. The different ring structure of BTX-A makes it more flexible than BTX-B, hence reducing its crystallinity and lead to broadened ^1H NMR signals. In the following we present results of our independent structural studies on brevetoxin-A (BTX-A), which after proposals of a transitional working structure,[10-12] arrived

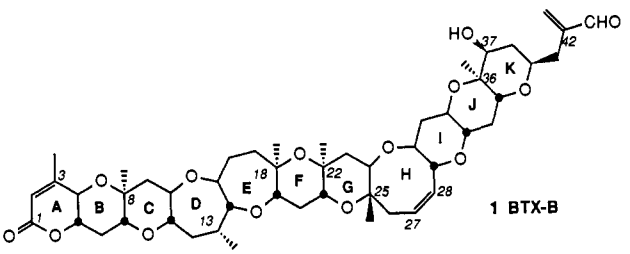

1 BTX-B

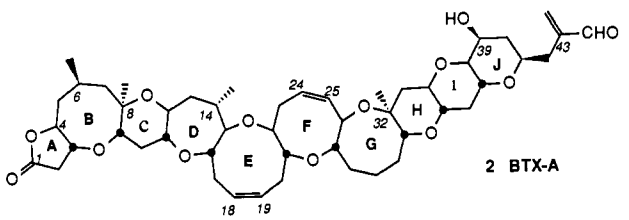

2 BTX-A

[†] Columbia University.
[‡] Suntory Institute for Bioorganic Research.
[§] University of Nebraska.
[⊥] Current address: Department of Chemistry, University of Missouri, Columbia, MO 65211.

(1) Shimizu, Y. *Marine Natural Products*; Scheuer, P. J., Ed.; Academic Press: New York, 1978; Vol. 1, Chapter 1.
(2) Taylor, D. L.; Seliger, H. H. *Toxic Dinoflagellate Blooms*; Elsevier/North-Holland: New York, 1979.
(3) Baden, D. G.; Bikhazi, G.; Decker, S. J.; Foldes, F. F.; Leung, I. *Toxicon* **1984**, *22*, 75-84 and references cited therein.
(4) Lin, Y.; Risk, M.; Ray, S. M.; Van Engen, D.; Clardy, J.; Golik, J.; James, J. C.; Nakanishi, K. *J. Am. Chem. Soc.* **1981**, *103*, 6773-6775.
(5) Golik, J.; James, J. C.; Nakanishi, K.; Lin, Y. Y. *Tetrahedron Lett.* **1982**, *23*, 2535-2538.
(6) Chou, H. N.; Shimizu, Y. *Tetrahedron Lett.* **1982**, *23*, 5521-5524.
(7) Chou, H. N.; Shimizu, Y.; Van Duyne, G.; Clardy, J. *Tetrahedron Lett.* **1985**, *26*, 2865-2868.
(8) There has been confusion in the nomenclature of these toxins. See footnote 7 in ref 9 and also ref 10.
(9) Shimizu, Y.; Chou, H. N.; Bando, H.; Van Duyne, G.; Clardy, J. C. *J. Am. Chem. Soc.* **1986**, *108*, 514-515.
(10) Nakanishi, K. *Toxicon* **1985**, *23*, 473-479.
(11) Tempesta, M. S.; Golik, J.; James, J. C.; Nakanishi, K.; Pawlak, J.; Iwashita, T.; Gross, M. L.; Tomer, K. B. 19th ACS National Meeting, Springfield, MO, Nov. 1, 1984.
(12) Tempesta, M. S.; Golik, J.; James, J. C.; Nakanishi, K.; Pawlak, J.; Iwashita, T.; Gross, M. L.; Tomer, K. B. The 1984 International Chemical Congress of Pacific Basin Societies, Honolulu, HI, Dec 16-21, 1984; Abstr. 10E 45.

0002-7863/87/1509-1144$01.50/0

at the same structure **2**[13] except for the 6-methyl configuration which was deduced as being α rather than β. In the following we describe how this challenging structure was constructed from combined nuclear magnetic resonance spectroscopy (NMR) and mass spectroscopy (MS) data of BTX-A and two derivatives **4** and **5**.

BTX-A was obtained in pure form in 1981[4] from the unialgal cultures of *G. breve* which were isolated during an outbreak at Florida in 1981; a 50-L culture containing 5×10^8 cells gave 0.8 mg of BTX-A, 5.0 mg of BTX-B, and 0.4 mg of BTX-C. The ichthyotoxicities (LC_{50}) against the fresh water zebra fish *Brachydanio rerio*, 0.2–0.6 g of body weight, in 1 h were as follows: BTX-A 3 ng/mL, BTX-B 16 ng/mL, and BTX-C 30 ng/mL; BTX-A is thus the most toxic of the three.[4,10] Preliminary studies on BTX-A showed it to possess a γ-lactone instead of the δ-enelactone in BTX-B; i.e., the skeletal structure was different. However, structural studies were hampered by the lack of material, susceptibility to air-oxidation (this instability being common to other toxins of this series), failure to secure crystals suitable for X-ray studies, etc.

Brevetoxin A (BTX-A) (**2**) ($C_{49}H_{70}O_{13}$) (molecular formula by high resolution fast atom bombardment MS, HRFABMS, see below), exhibited strong IR bands (KBr pellet) at 1791 (γ-lactone) and 1691 cm^{-1} (enal, also present in BTX-B). The UV (MeOH) had a maximum at 208 nm (ϵ 11 000; π,π^* of enal) accompanied by a shoulder at 215 nm (ϵ 8700; n,π^* of lactone), while the CD (MeOH) exhibited three extrema: 213 nm ($\Delta\epsilon$ − 1.64; n,p^* of lactone), 235 nm ($\Delta\epsilon$ + 1.23; assignment unclear), and 329 nm ($\Delta\epsilon$ + 0.15; n,π^* of enal). The UV and CD data of BTX-A (as well as BTX-B[4]) are unique in that many of them are complementary. Namely, the strongly UV-absorbing π,π^* transition of the enal moiety does not give rise to a detectable CD Cotton effect (CE) while the transitions leading to the appearance of CE's are not detectable in the UV. The CE due to the enal π,π^* band is presumably weak because the chromophore is removed by one methylene group from the chiral center; it is thus overlaid by the 213-nm CE of the lactone group in BTX-A and by the 225-nm CE of the enelactone group in BTX-B. The n,π^* transition of the enal moieties in BTX-B[4] and A both give rise to similar weakly positive CE's at 329 nm, +0.16 and +0.15, respectively; the fact that the signs are positive in both cases shows that the absolute configuration of the enal moieties are the same. Since the absolute configuration of BTX-B (**1**) was based on the application of the exciton chirality method[4] that of BTX-A should be as represented by structure **2**.

The ^{13}C NMR spectrum ($CDCl_3$) indicated the presence of four methyls at δ 27.6, 21.3, 16.7, and 15.0 ppm, a 1,1′-disubstituted ene at δ 148.0 (s, C-43)/136.0 ppm (t, C-45), four 1,2-disubstituted enes at δ 138.6 (d), 129.3 (br d), 126.7 (br d), and 124.3 (d) ppm, a lactone carbonyl at 172.4 ppm, and an aldehyde at 194.4 ppm. In addition, seventeen C–O signals were observed at 92.1 (br d), 87.0 (d), 85.0 (d), 84.9 (d), 83.5 (br d), 81.7 (d), 79.8 (d), 79.4 (d), 78.5 (d), 77.4 (d), 76.8 (s), 76.0 (s), 71.5 (br d), 71.0 (d), 69.1 (d), 66.0 (d), 62.1 ppm (d), thirteen CH_2's at *52.8* (C-7), 45.1, 43.2, 37.7, 37.6, 35.5, 35.3, 34.4, 33.5, 31.6, 31.0 (br), 28.8 (br), *19.4* (br, C-29), and two CH's at 36.5 and 27.3 (br) ppm. Thus 44 of the 49 carbons in BTX-A could be identified.

Two features of the ^{13}C spectra were notable, a concentration- and temperature-dependent broadening of certain lines (signals designated "br" above), and two methylene signals with unusual chemical shifts (italicized above). The line broadening observed in ^{13}C NMR spectra was also present in the ^1H NMR spectra and was thought to be due to conformational isomers present in solutions at 25 °C (Figure 2a). This was the first indication of the presence of medium-sized rings in BTX-A. The unusually low chemical shift of the methylene at 52.8 ppm showed that it had to be heavily β-substituted (C-7, see Figure 1a), whereas the high chemical shift of the other methylene at 19.4 ppm required

(13) Nakanishi, K.; Pawlak, J. ACS National Meeting, New York, NY, April 13–18, 1986; Abstr. ANAL 0049.

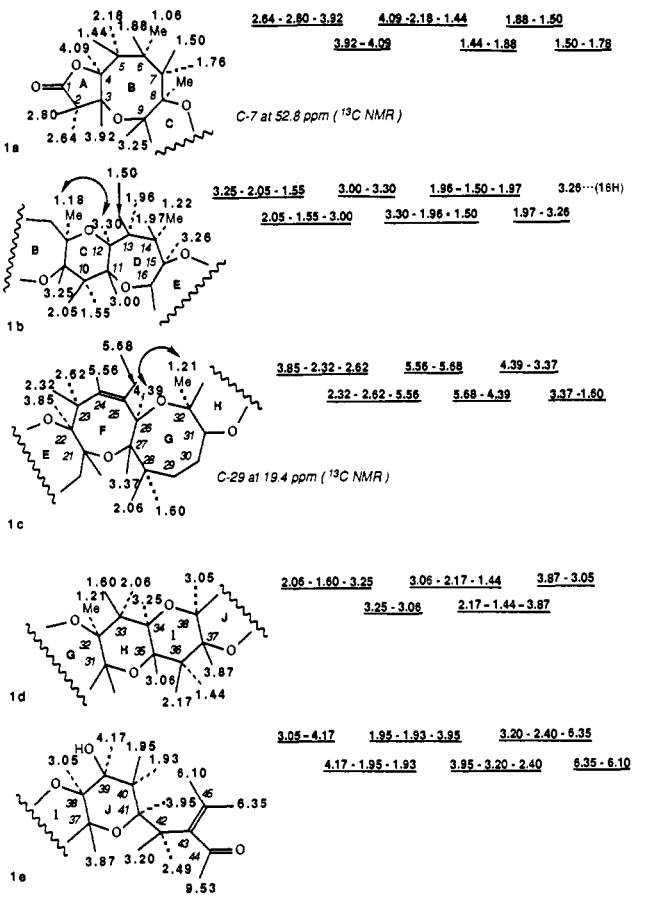

Figure 1. Summary of proton assignments obtained from COSY on BTX-A in $CDCl_3$ and $CDCl_3$/benzene-d_6.

it to be in an isolated environment and subject to multiple γ-effects (C-29, see Figure 1c).

The outcome of NMR experiments COSY, decoupling, and difference nuclear Overhauser effect (DnOe) are summarized in structures **2a** and **2b** (Figure 2) derived on the basis of NMR data. The NMR studies clarified the relative stereochemistry of BTX-A as well, showing that it has a trans fused ring system similar to that found in BTX-B. One of the main drawbacks in the COSY sequence is that the technique fails to define connectivities between protons with very similar chemical shifts. However, the assignments became feasible by comparing COSY maps obtained under various mixtures of $CDCl_3$ and C_6D_6. The COSY experiments were thus performed in $CDCl_3$ (Figure 1), $CDCl_3$–C_6D_6 (1:1), and C_6D_6 (Figure 2). Another problem encountered was excessive line broadening due to conformational equilibria where COSY failed to clarify connectivities of protons with broad signals; however, this was overcome by homonuclear decoupling studies carried out at elevated temperatures.

NMR Studies (Figures 1 and 2). The sheer number of protons (70) made the NMR complex; however, as it turned out, the fact that the contiguous oxacyclic skeleton consisted of a single carbon chain with no branching except for two sec-methyls (C-6 and C-14) and two tert-methyl groups (C-8 and C-32) was a simplifying factor in elucidating the proton connectivities through 2D COSY and decoupling experiments. The latter two methyls also broke the carbon chain into three shorter chains, C-1 through C-7, C-9 through C-31, and C-33 through C-44. The numerals in the following text refer to chemical shifts in $CDCl_3$ (Figure 1).

(a) Rings A and B (Figure 1a). The proton signals which were found to be connected are linked by an underline in the following sequence

2.64 − 2.80 − 3.92 4.09 − 2.18 − 1.44 1.88 − 1.50

3.92 − 4.09 1.44 − 1.88 1.50 − 1.78

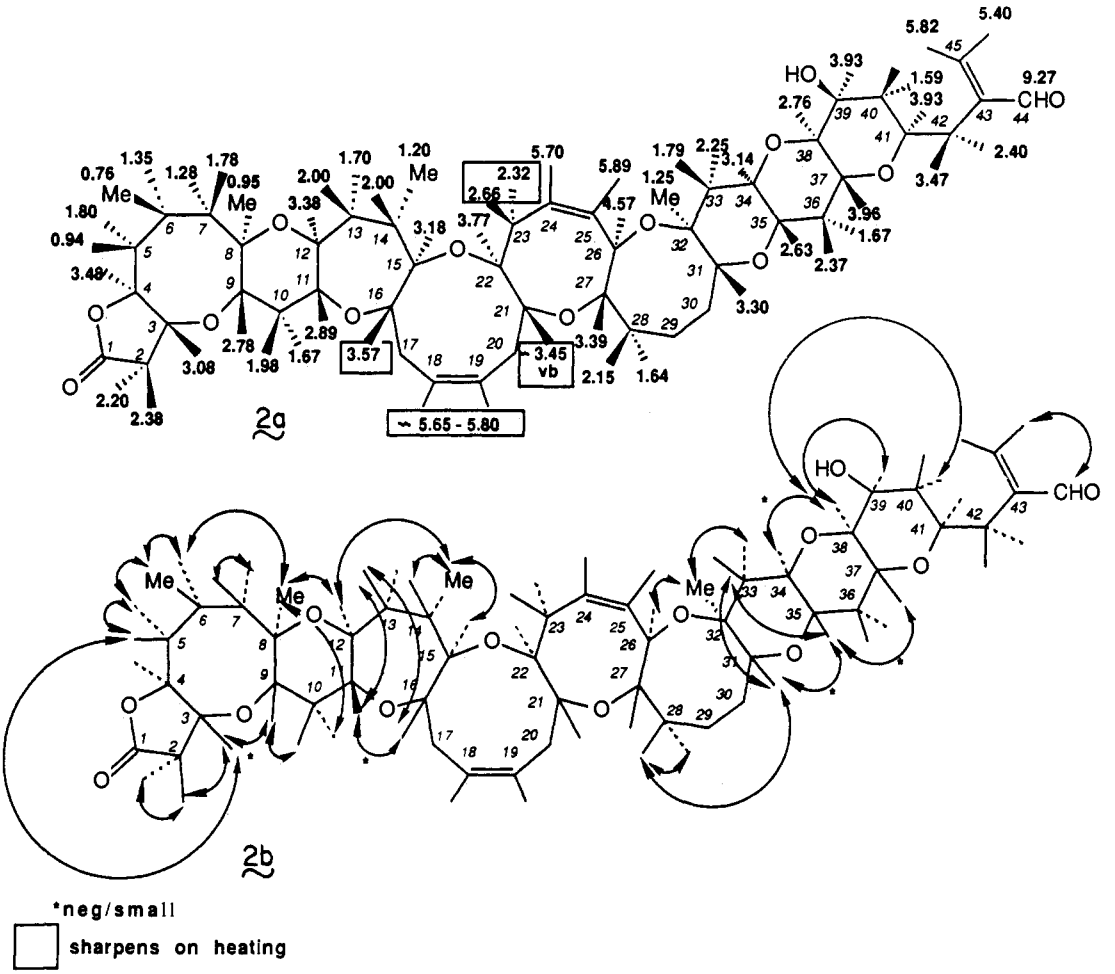

Figure 2. Summary of ^{1}H NMR studies, COSY, difference NOE, and high-temperature decoupling in benzene-d_6.

No further coupling of the 1.50/1.78 signals were observed, thus suggesting a quaternary carbon at the B/C ring juncture. There are only two methyl singlets observed in the ^{1}H NMR spectrum at δ 1.18 and 1.21; the downfield methyl is attached to C-32 (see below) while the upfield methyl is shown to be attached to C-8 from its NOE to 10 α-H and 12 α-H (Figure 2). The other NOE's depicted in Figure 2 clarify the stereochemistry of A/B/C ring junctures. Although assignments for the protons have been made above, evidence for the eight-membered nature of ring B was secured from MS data (below).

The wrong assignment of a 6α-stereochemistry to the 6-Me was based on the assumption that the eight-membered ring B had twist-boat crown conformation (i). Irradiation of a signal at δ

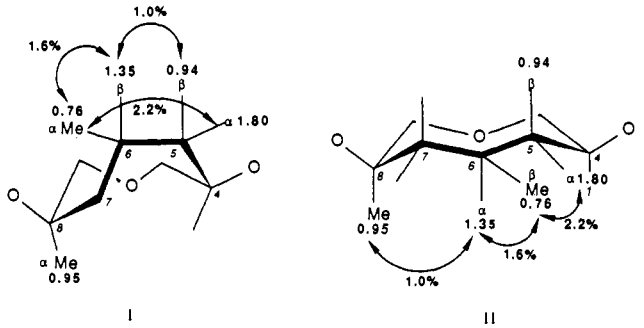

0.94 (assigned to 5β-H) induced an NOE to a 6-H signal at δ 1.35, thus implying that its configuration was 6β, or 6-Me was α. However, the X-ray crystallography of BTX-A derivative[7] shows that the eight-membered ring B is in crown conformation (ii). From this it is evident that the NOE observed was actually that between the 8-Me at δ 0.95 and the 6-H at δ 1.35; 6-H is therefore α and 6-Me is β. It is interesting to note that the eight-membered cyclic ether (ring B) adopted the unfavorable crown conformation. This exemplifies the difficulty in substantiating conformation of medium-sized rings.

(b) Rings C and D (Figure 1b).

$$\underline{3.25 - 2.05 - 1.55}\quad \underline{3.00 - 3.30}\quad \underline{1.96 - 1.50 - 1.97}\quad 3.26 \cdots$$
$$\underline{2.05 - 1.55 - 3.00}\quad \underline{3.30 - 1.96 - 1.50}\quad \underline{1.97 - 3.26}$$

Difference NOE between the δ 1.18 methyl and the 3.30 methine signals enabled one to link moieties A/B and B/C/D. Small coupling of $J < 1$ Hz was observed between 14-H (δ 1.97) and 15-H (δ 3.26) indicating that the dihedral angle is close to 90° (Figure 1b). This fact plus the NOE observed between 14-Me/15-H and between 14-Me/12-H suggests all of them to be α (Figure 2, the 12-H further exhibits an NOE between 8α-Me). Neither the 15-H (δ 1.97)/16-H coupling nor the 16-H signal could be detected due to line broadening at 25 °C. However, high-temperature ^{1}H NMR studies in benzene-d_6 clearly located 16-H at δ 3.57 (Figure 2a); at 45° in benzene-d_6, homonuclear decoupling of the 15-H (δ 3.18) clearly showed coupling to 14-H (δ 2.00) as well as to 16-H (δ 3.57). This 16-H assignment was further substantiated by the observed difference NOE (1%, 25°, benzene-d_6) upon irradiation of 11-H (δ 2.89).

(c) Rings F and G (Figure 1c).

$$\underline{3.85 - 2.32 - 2.62}\quad \underline{5.56 - 5.68}\quad \underline{4.39 - 3.37}$$
$$\underline{2.32 - 2.62 - 5.56}\quad \underline{5.68 - 4.39}\quad \underline{3.37 - 1.60}$$

The 5.68-ppm 25-H peak (dd, J = 4 and 10 Hz) constitutes a cis-disubstituted ene with the 5.56-ppm 24-H peak. An NOE between δ 4.39 (26-H) and a methyl singlet at δ 1.21 (32-Me) was observed, but the remaining protons in ring H could not be identified due to substantial chemical shift overlap and line

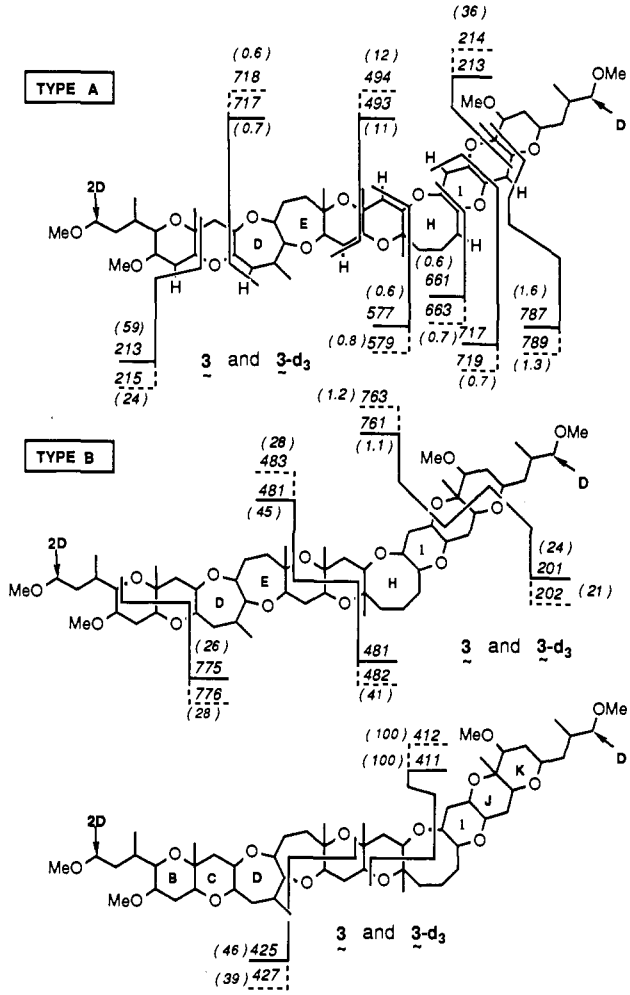

Figure 3. Ions formed by type A and type B fragmentations as observed in the mass spectra of 1,5,37,42-tetra-*O*-methyldodecahydrobrevetoxin-B (**3**) and its 1,1,42-trideuterio analogue **3**-d_3.

broadening. The ring size was determined to be eight-membered by MS studies (see below).

(d) Rings H and I (Figure 1d).

2.06 - 1.60 - 3.25 3.06 - 2.17 - 1.44 3.87 - 3.05

3.25 - 3.06 2.17 - 1.44 - 3.87

No further coupling is observed, suggesting C-32 is quaternary, bearing a methyl substituent (this follows from the presence of two methyl singlets in ^{1}H NMR and two quaternary carbons in ^{13}C NMR). This connectivity indicates rings H and I are both fused tetrahydropyran rings.

(e) Enal and Ring J (Figure 1e).

3.05 - 4.17 1.95 - 1.93 - 3.95 3.20 - 2.40 - 6.35

4.17 - 1.95 - 1.93 3.95 - 3.20 - 2.40 6.35 - 6.10

The structure of the three terminal rings H/I/J and the enal moiety is similar to that in BTX-B (BTX-A has no angular methyl between rings I/J). The small coupling of 39-H and 41-H to the adjacent 40-methylene protons shows that both methine hydrogens are equatorial; 39-OH is hence axial as in the case of the 37-OH in BTX-B.

(f) Ring E. The central portion of BTX-A proved impossible to assign by COSY due to line broadening caused by conformational flexibility. This is also seen in the ^{13}C spectrum where some peaks, e.g., δ 126.7 and δ 129.2 are broadened depending on the concentration, solvent, and temperature. This suggests that the central moiety is a medium-sized ring. The ^{1}H NMR also showed a very broad vinyl peak (2 H) centered at δ 5.56 which sharpened upon heating. Little information remained in the $CDCl_3$ COSY maps regarding ring E and placement of the remaining ene.

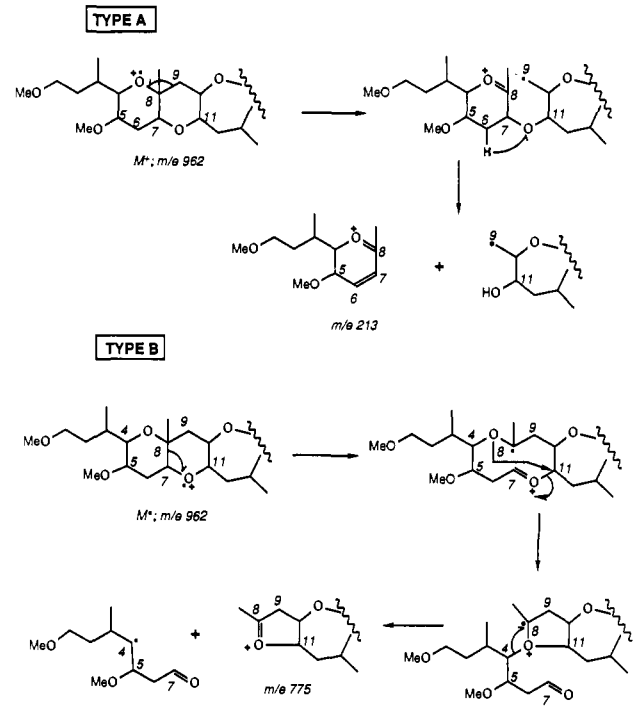

Figure 4. Proposed fragmentation pathway for the formation of type A (*m/e* 213) and type B (*m/e* 775) fragment ions observed in the mass spectrum of 1,5,37,42-tetra-*O*-methyldodecahydrobrevetoxin-B (**3**).

High-temperature proton studies using homonuclear decoupling experiments as well as ambient COSY and DNOE were performed in benzene-d_6. This allowed most of the remaining protons to be assigned and gave a more complete picture of the ring connectivity and stereochemistry. The chemical shifts and NOE's are summarized in Figure 2. The NOE's allowed rings B/C and G/H to be unequivocally joined and showed the ring system to be trans fused as in the other brevetoxins. The stereochemistry of 6-Me and location of the double bond in rings E and F remained unclear from NMR studies. However, these and other structural aspects, except for the 6-Me configuration, could be elucidated from MS studies.

MS Studies (Figures 3–7). (a) BTX-B 1 (Figures 3 and 4). MS studies of BTX-A were carried out by using BTX-B (**1**) as model. In order to obtain a compound suitable for EI (electron impact)-MS analysis, BTX-B was derivatized by the following scheme: 1. Catalytic hydrogenation of the three double bonds to form 2,3,27,28,41,43-hexahydro-BTX-B. 2. Reduction with sodium borohydride or sodium borodeuteride to yield dodecahydro-BTX-B or its 1,1,42-trideuterio analogue with an opened lactone ring (west side) and reduced aldehyde (east side). 3. Methylation with methyl iodide and sodium hydride of the four hydroxyl groups to form 1,5,37,42-tetra-*O*-methyldodecahydro-BTX-B (**3**) and its trideuterio analogue (**3**-d_3).

The BTX-B derivatives **3** and **3**-d_3 thus prepared were analyzed by EIMS. Mass spectra of **3** and **3**-d_3 showed molecular ions at *m/e* 962 (0.6%) and 965 (0.7%), respectively, the latter showing incorporation of three deuterium atoms.

The ions formed by simple fragmentation of the molecular ions of **3** and **3**-d_3 are as follows: 1. *m/e* 962 → *m/e* 947 → *m/e* 915 in **3** and *m/e* 965 → *m/e* 950 → *m/e* 918 in **3**-d_3, formed by losses of methyl radical and then methanol. 2. *m/e* 962 → *m/e* 930 → *m/e* 898 in **3** and *m/e* 965 → *m/e* 933 → *m/e* 901 in **3**-d_3, formed by sequential elimination of two methanol molecules.

Most of the fragment ions in the MS of **3** and **3**-d_3 originate from two ether type fragmentation pathways which from this point forward will be called type A and type B fragmentations. The two series of fragment ions are depicted in Figure 3. Both type A and type B fragmentations, shown in Figure 4, begin with homolytic cleavage of one of the carbon–carbon bonds adjacent to the ionized oxygen. Thus formation of the ion at *m/e* 213 (type

Table I. HRMS Data of the Selected Ions from the Mass Spectrum of 1,4,39,44-Tetra-*O*-methyldodecahydrobrevetoxin-A (**4**)

m/e	acc mass	elem comp	*m/e*	acc mass	elem comp
151	151.1122	$C_{10}H_{15}O$	465	465.3212	$C_{27}H_{45}O_6$
181[a]	181.1234	$C_{11}H_{17}O_2$	481	481.3183	$C_{27}H_{45}O_7$
183	183.1376	$C_{11}H_{19}O_2$	537	537.3775	$C_{31}H_{53}O_7$
213[a]	213.1485	$C_{12}H_{21}O_3$	579	579.3872	$C_{33}H_{55}O_8$
215	215.1636	$C_{12}H_{23}O_3$	591	591.3905	$C_{34}H_{55}O_8$
245	245.1749	$C_{13}H_{25}O_4$	621	621.4371	$C_{36}H_{61}O_8$
313	313.2029	$C_{17}H_{29}O_5$	647	647.4534	$C_{38}H_{63}O_8$
325	325.2015	$C_{18}H_{29}O_5$	663	663.4476	$C_{38}H_{63}O_9$
355	355.2474	$C_{20}H_{35}O_5$	703	703.4777	$C_{41}H_{67}O_9$
367	367.2487	$C_{21}H_{35}O_5$	719	719.4740	$C_{41}H_{67}O_{10}$
397	397.2594	$C_{22}H_{37}O_6$	745	745.4926	$C_{43}H_{69}O_{10}$
453	453.3204	$C_{26}H_{45}O_6$			

[a] These two ions are due to sequential loss of methanol from the ion at *m/e* 245.

A, Figure 4) is initiated by cleavage of the C-8/C-9 bond and subsequent cleavage of the C-7/O bond with simultaneous transfer of 6-H to 11-O. An example of a type B fragmentation leading to ion at *m/e* 775 is shown in Figure 4. It is created by cleavage of the C-7/C-8 bond with formation of a radical at C-8; this species is further transformed by concurrent formation of an aldehyde group at C-7 and a carbocation at C-11; this is immediately stabilized by formation of a cyclic oxonium ion. The last step is homolytic cleavage of the C-4/O bond to form the ion at *m/e* 775; note the five-membered oxonium ring is now one size smaller than the starting ring C.

Deuteriation introduced two D's in the west terminal and one D in the east terminal of the molecule; thus the deuteriation shifts shown in Figure 3 indicate the direction of ion formation and substantiate the proposed fragmentation pattern. Clarification of the two fragmentation mechanisms and the fact that the four methoxyl oxygens 1-O/5-O/37-O/42-O are not part of the oxacyclic system led to the finding of an important relationship between the degree of unsaturation in a given fragment ion and the number of oxygens in that ion. (i) In type A fragments, the degree of unsaturation is one less than the number of oxygens in that ion, e.g., for *m/e* 213 cation $C_{12}H_{21}O_3$ having three oxygens the unsaturation number is 2 (the double bond linked to the oxonium ion is not considered an unsaturation, Figure 4). Since the terminal ring in type A fragments always carry one double bond, the total number of rings is one less than the unsaturation number. Moreover, the ring size of the oxonium ring remains the same as in the original compound. (ii) In type B fragments, the degree of unsaturation number is two less than the number of oxygens contained in the ion, e.g., for *m/e* 775 cation (Figure 4) $C_{44}H_{71}O_{11}$ having 11 oxygens the degree of unsaturation is 9. The degree of unsaturation and the number of rings are identical. The ring size of the oxonium ring is contracted by one carbon as compared to the original compound. These two relations (i) and (ii) and the information supplemented by NMR on the location of methyl groups made it possible to reconstruct the structure of BTX-B. In the case of the unknown BTX-A derivatives **4** and **5**, the rules and elemental compositions of cations not only led to facile distinction between type A and type B fragments but also more crucially allowed one to derive the oxacyclic skeletal structure itself (see below).

(b) BTX-A 2 (Figure 5–7, Tables I and II). High-resolution fast atom bombardment mass spectroscopy (HRFABMS) of BTX-A (**2**) led to an $[M + H]^+$ ion at *m/e* 867.4885 ($C_{49}H_{71}O_{13}$, calcd 867.4894). The degree of unsaturation 15 calculated from the elemental composition, together with the presence of a γ-lactone, an enal and two double bonds showed that **2** contains ten rings. As in the previous case, BTX-A was derivatized as follows: 1. Reduction of the lactone and aldehyde group with sodium borohydride to form hexahydro-**2**. 2. Hydrogenation of the three double bonds to form dodecahydro-**2**. 3. Methylation of the four hydroxyl groups with methyl iodide and sodium hydride to form 1,4,39,44-tetra-*O*-methyl-dodecahydro-BTX-A (**4**).

The EIMS shows an M^+ ion at *m/e* 934 (19.0%), i.e., $C_{53}H_{90}O_{13}$, in agreement with the well-defined chemical transformations leading to **4**. This suggested the presence of nine fused cyclic ether rings. The ions formed by simple fragmentation of the molecular ion are as follows: *m/e* 934 → *m/e* 919 loss of methyl radical; *m/e* 934 → *m/e* 916 loss of water; *m/e* 934 → *m/e* 902 loss of methanol.

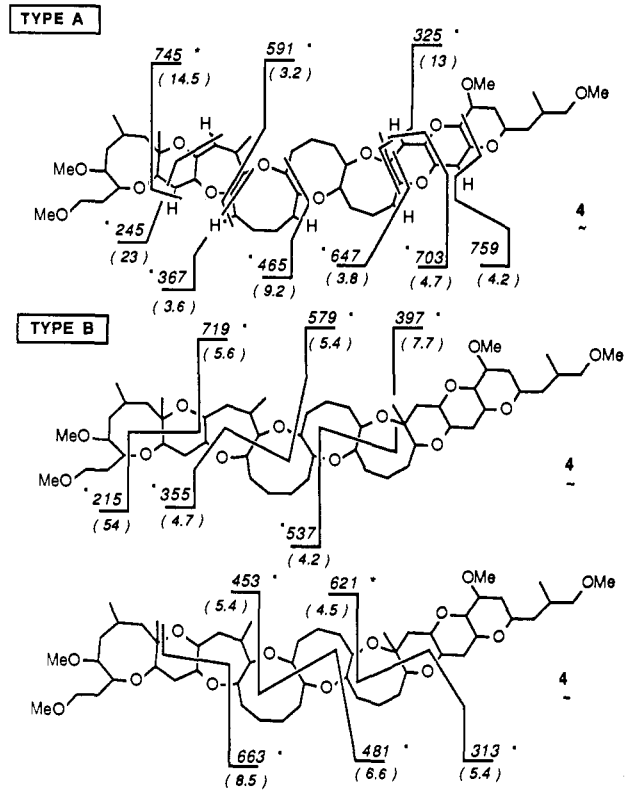

Figure 5. Ions formed by type A and type B fragmentations as observed in the mass spectrum of 1,4,39,44-tetra-*O*-methyldodecahydrobrevetoxin-A (**4**). Asterisks (*) denote peaks which were analyzed by HRMS (Table I).

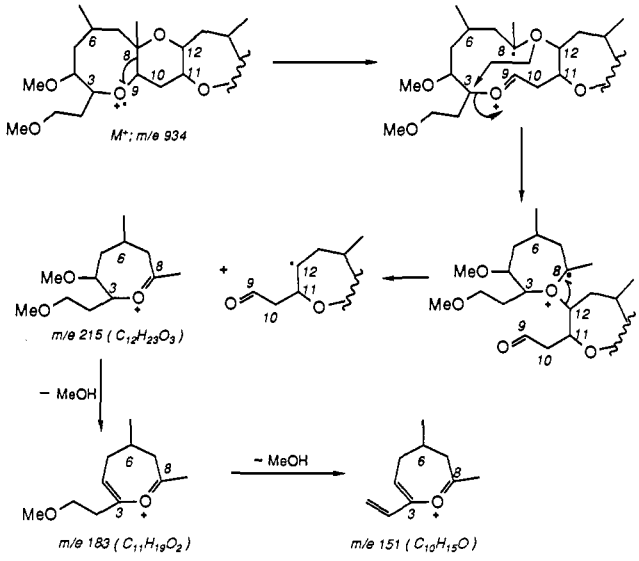

Figure 6. Proposed fragmentation pathway for the formation of type B (*m/e* 215) fragment ion observed in the mass spectrum of 1,4,39,44-tetra-*O*-methyldodecahydrobrevetoxin-A (**4**).

Type A and type B fragment ions are depicted in Figure 5, the elemental compositions of pertinent cations being determined by HRMS (Table I) in order to apply rules (i) and (ii) for the construction of structure **4**. The ion *m/e* 215 ($C_{12}H_{23}O_3$) enabled us to start construction of **4** from its west end or ring B (Figure 6). The degree of unsaturation (1) calculated from the elemental composition and the number of oxygens (3) indicated it to be a type B fragment (rule ii). Moreover, the degree of unsaturation

of the cation shows it to be monocyclic, the size of the ring being deduced as follows: (a) The *m/e* 215 ion undergoes two sequential losses of methanol yielding ions at *m/e* 183 ($C_{11}H_{19}O_2$) and 151 ($C_{10}H_{15}O$); this leaves 10 carbon atoms to be accounted for. (b) The presence of BTX-A of a terminal γ-lactone (NMR, IR) accounts for two more carbons C-1 and C-2 in the *m/e* 151 fragment, thus leaving 8 carbons for further consideration. (c) 2D NMR spectral data (see NMR section) enabled one to place two methyl groups on ring B; this results in a seven-membered oxacarbocyclic oxonium ion containing 6 annular carbons.

Since the oxonium ring is one size smaller in type B fragments (rule ii), the original ring B in **4** (and in BTX-A **2**) is deduced to be eight-membered. The structure of ring B is further corroborated by the presence of type A ions at *m/e* 245 ($C_{13}H_{25}O_4$) and 745 ($C_{43}H_{69}O_{10}$) in the MS of **4**.

Construction of rings C and D will be discussed next. a. In ion *m/e* 719 ($C_{41}H_{63}O_{10}$) iii the degree of unsaturation is 8 and therefore is a type B fragment (rule ii); similarly, the ion *m/e* 663 ($C_{38}H_{63}O_9$) iv has 7 degrees of unsaturation and is also a type

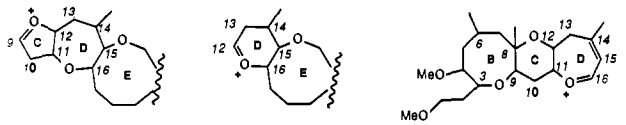

B fragment (see Figure 5). The number of rings present in these ions make it clear that the two fragments involve ring C. b. The ion iii contains three more carbons than iv. In type B fragmentations, the ring juncture carbon adjacent to the oxygen which is originally ionized is lost, i.e., in iv C-11 is lost. Therefore, the terminal ring in iii or the oxonium ring derived from ring C must be five-membered; thus, in original compound **4**, ring C is six-membered. c. Type A ion at *m/e* 367 ($C_{21}H_{35}O_5$) v has an unsaturation number of 4, and since the terminal ring in type A fragments has one double bond, it follows that *m/e* 367 consists of three rings. The moieties involving rings B and C (eight- and six-membered ring, respectively) have been clarified above. Thus, this leaves only ring D for clarification. From NMR data it is evident that one sec-Me is present in this ring. With this information at hand we were able to deduce the ring size of ring D as being 7.

The structure of ring E is derived in a straightforward manner from the two type A ions *m/e* 591 and 465 (Figure 5) and the knowledge that the two sec-Me's in BTX-A are attached to C-6 and C-14. Site of the methyl group at the B/C juncture is deduced as follows. Type A ion at *m/e* 745 ($C_{43}H_{69}O_{10}$) vi contains eight (9 deg of unsaturation) rings including ring C. Type B ion at *m/e* 719 ($C_{41}H_{67}O_{10}$) vii also contains eight rings (8 deg of unsaturation) including ring C, the size of the terminal ring C differing by one carbon (rules i and ii). However, vi has two more carbons

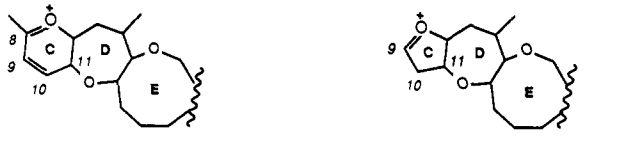

than vii. The extra carbon therefore has to be linked to C-8. The angular methyl at C-32 can be located in an identical manner by consideration of ions *m/e* 647 ($C_{38}H_{67}O_8$) (type A) and *m/e* 621 ($C_{36}H_{61}O_8$) (type B). The remainder of the molecule **4** can be constructed entirely in a similar fashion by considering the two types of fragmentations and additional data from NMR.

The location of double bonds in BTX-A was determined from MS studies of another derivative, namely the ozonolysis product **5**, and prepared as follows: 1. Reduction of the γ-lactone and aldehyde group with sodium borohydride. 2. Ozonolysis of the three double bonds. 3. Reduction of ozonides with sodium borohydride. 4. Methylation of hydroxyl groups with methyl iodide and sodium hydride to form BTX-A derivative **5**.

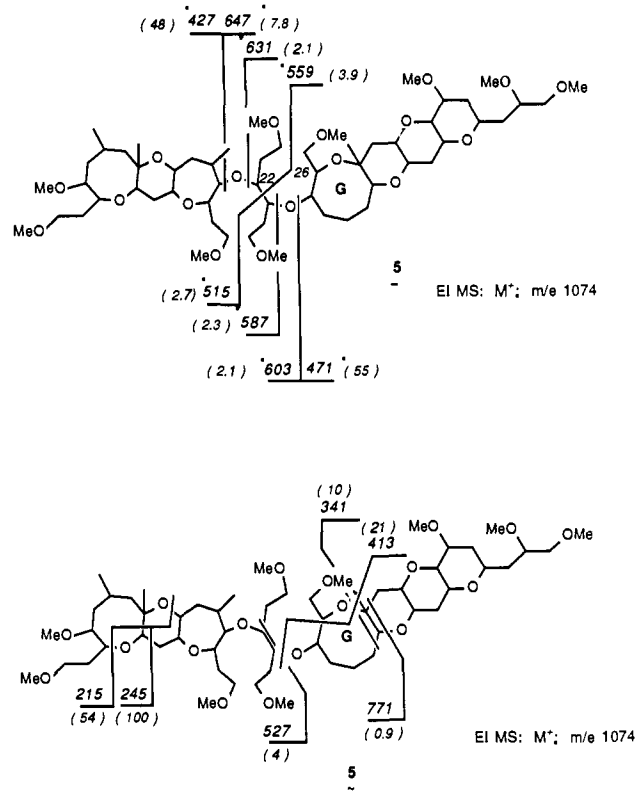

Figure 7. Fragmentation pattern of ozonolysis derivative of BTX-A (**5**) diagnostic for location of double bonds in BTX-A (**2**). Type A and type B fragmentation patterns are also observed in the mass spectrum of ozonolysis derivative 5. Asterisks (*) denote peaks which were analyzed by HRMS (Table II).

Table II. HRMS Data of the Selected Ions from the Mass Spectrum of Ozonolysis Derivative of BTX-A (**5**)

m/e	acc mass	elem comp	*m/e*	acc mass	elem comp
427	427.3065	$C_{24}H_{43}O_6$	587	587.4165	$C_{32}H_{59}O_9$
471	471.2964	$C_{25}H_{43}O_8$	603	603.4115	$C_{32}H_{59}O_{10}$
515	515.3591	$C_{28}H_{51}O_8$	631	631.4062	$C_{33}H_{59}O_{11}$
559	559.3487	$C_{29}H_{51}O_{10}$	647	647.4011	$C_{33}H_{59}O_{12}$

The molecular ion at *m/e* 1074 (rel % 5.9) is in accord with the product expected from these reactions. A plausible fragmentation path for formation of an ion at *m/e* 998 (rel% 7.5) begins with loss of methoxymethylene radical from C-26 followed by loss of methoxy radical. Genesis of an ion at *m/e* 984 (rel% 4.5) can be explained similarly by loss of methoxyethylene radical from C-22 followed by loss of methoxy radical. The crucial fragment ions formed by single bond ether cleavages (Figure 7), the elemental compositions of which were determined by HRMS (Table II), established the location of the two 1,2-disubstituted double bonds in BTX-A. The *m/e* 427 ion ($C_{24}H_{43}O_6$) indicated that a $-CH_2CH_2OCH_3$ group is at C-16 as a result of ozonolysis, reduction, and subsequent methylation. This places the ene at C-18/C-19 in ring E; the remaining cations shown in Figure 7 are all in agreement with the C-18/C-19 and C-24/C-25 ene locations. Ozonolysis product **5** also underwent type A and B fragmentations (Figure 7).

Experimental Section

Spectroscopic Measurements. The COSY and difference NOE spectra were obtained at 360 MHz on a Nicolet NT-360 NMR spectrometer equipped with NIC 1280/293B data system. COSY spectra, difference NOE, and high-temperature studies were also performed at 500 MHz in benzene-d_6, Bruker AM-500 instrument. The spectra were measured at 25 °C by using a 5-mm probe with an internal D lock, 90° (H) pulse width 5.9 μsec. The COSY maps were acquired by using a 16-step Jeener pulse sequence with phase alternation: 90° (H)-t_1-90°(H)-t_2.[14]

(14) Bax, A.; Freeman, R.; Morris, G. *J. Magn. Reson.* **1981**, *42*, 164–168.

High-resolution electron impact spectra were obtained on a Kratos MS-50 by using a direct insertion probe. Instrument conditions were as follows: ionizing energy, 70 eV; accelerating potential, 8 KeV; source temperature, 250 °C. Fast atom bombardment spectra were obtained on a Kratos MS-50TA.[15] An Ion Tech atom gun and a standard Kratos FAB source were used. The samples were dissolved in thioglycerol, and a small drop of the sample solution was placed on the copper target of the FAB direct insertion probe. The sample was bombarded with 8 keV xenon atoms, and the ions produced were accelerated through 8 keV.

Reduction with Sodium Borohydride or Sodium Borodeuteride (Procedure a). BTX-B or BTX-A (5 mg) was dissolved in methanol (1 mL) and allowed to stand with slight excess of sodium borohydride or sodium borodeuteride for 15 min at room temperature. Reaction mixture was treated with Dowex 50 W × 8 (H^+), filtrated, and evaporated to dryness. The residue was twice evaporated with methanol.

Catalytic Hydrogenation (Procedure b). The compound to be hydrogenated (5 mg) was dissolved in THF (1 mL) and hydrogenated (4 h, room temperature) over 10% Pd/C (2 mg) under a slight hydrogen pressure. The catalyst was centrifuged, and the supernatant was evaporated to dryness.

Methylation (Procedure c). The compound to be methylated (4 mg) was dissolved in THF (1 mL) and stirred with sodium hydride for 20 min. Methyl iodide (0.05 mL) was then added. After 16 h *n*-hexane (5 mL) was added, the mixture was centrifuged, and the supernatant was evaporated to dryness.

(15) Gross, M. L.; Chess, E. K.; Lyon, P. A.; Crow, F. W.; Evans, S.; Judge, H. *Int. J. Mass Spectrum Ion Phys.* **1982**, *42*, 243-254.

1,5,37,42-Tetra-*O*-methyldodecahydrobrevetoxin-B (3) and Its 1,1,42-Trideuterio Analogue (3-d_3). BTX-B (5 mg) was hydrogenated by procedure b, reduced with sodium borohydride or sodium borodeuteride by procedure a, and finally methylated by procedure c. The product obtained (**3** and **3**-d_3) was purified by flash chromatography with benzene-ethyl acetate (1:1) and analyzed by EIMS.

1,4,39,44-Tetra-*O*-methyldodecahydrobrevetoxin-A (4). BTX-A (5 mg) was reduced with sodium borohydride by procedure a, hydrogenated by procedure b, and finally methylated by procedure c. The product obtained (**5**) was purified by flash chromatography with benzene-ethyl acetate (1:1) and analyzed by EIMS.

BTX-A Ozonolysis Derivative 5. BTX-A (5 mg) was reduced with sodium borohydride by procedure a. The product obtained was dissolved in methanol (1 mL) and ozonized at -78 °C for 20 min. The solution was then purged by argon for 1 h. The ozonides formed were reduced with sodium borohydride by procedure a. The product obtained was methylated by procedure c and purified by flash chromatography with benzene-ethyl acetate 1:1.

Acknowledgment. We are grateful to Dr. John C. James for discussions and Joseph C. Cesarelli for technical assistance. The studies were supported in part by NIH Grant AI 10187 (to K.N.) and NSF Grant No. CHE-8211164 (to MCMS, an NSF Regional Instrumentation Facility).

Supplementary Material Available: Table of mass spectral data (7 pages). Ordering information is given on any current masthead page.

Kinetics, Stereochemistry, and Mechanism of Interaction of Vaska's Complex with Ethynylvinyl Triflates. Formation of Novel σ-Butatrienyl-Iridium Compounds

Peter J. Stang,*[1a] Vandana Dixit,[1a,b] Melvyn D. Schiavelli,[1c] and Paul Drees[1c]

Contribution from the Departments of Chemistry, The University of Utah, Salt Lake City, Utah 84112, and The College of William and Mary, Williamsburg, Virginia 23185.
Received August 15, 1986

Abstract: The reaction of Vaska's complex [$(Ph_3P)_2Ir(CO)(Cl)$, **3**] with a variety of substituted enynyl triflates [RCH=CH(OTf)C≡CR′, **4** and **5**] was investigated. Oxidative addition readily occurs in benzene or toluene at room temperature to give novel, isolable, crystalline hexacoordinate iridium(III) butatrienyl complexes **8**. Rate studies indicate steric inhibition by bulky substituents on the terminal acetylenic carbon and give high negative entropies of activation. A careful stereochemical investigation showed that reaction occurs with complete (or nearly complete) *retention* of olefin stereochemistry. A two-step S_N2' process with syn approach of the incoming Ir nucleophile is proposed to account for these observations.

Oxidative addition reactions are among the most ubiquitous and well-investigated processes in organometallic chemistry.[2] Particularly important and valuable oxidative additions are carbon-metal σ-bond-forming reactions, for they generally represent an obligatory step in the multitude of metal-mediated catalytic carbon coupling processes. A great variety of organic substrates such as alkyl,[2a,f] benzyl,[2f,3] allyl,[4] propargyl,[5] acyl,[2a,3] vinyl,[3,6] and aryl[2e,3] systems (usually halides) undergo oxidative additions, most often with d^8 and d^{10} metal complexes, with the metal generally serving as a nucleophile.

A good deal is known about the nature and mechanism of these reactions with alkyl, benzyl, allyl, acyl, and aryl halides, whereas the vinylic systems are much less investigated and understood.[2-7] This parallels the state of affairs in organic chemistry where aliphatic and aromatic nucleophilic substitutions (S_N1, S_N2, S_NAr, etc.) are well understood but until recently nucleophilic vinylic substitutions (S_NV) were generally ignored.[8] The reasons for this apparent anomaly are usually ascribed to the inertness of simple alkylvinyl halides to S_NV processes even with powerful nucleophiles or under forcing solvolytic conditions.[8]

The introduction of the perfluorosulfonate leaving groups, with a $k_{CF_3SO_3^-}/k_{X^-}$ reactivity ratio of 10^6-10^8, and the ready availability of vinyl triflates[9] ameliorates this difficulty, as illustrated by the easy generation of both simple alkylvinyl cations[10] and alkylide-

(1) (a) Utah. (b) Abstracted in part from: Dixit, V. *Ph.D. Dissertation* University of Utah, 1985. (c) William & Mary.
(2) (a) Collman, J. P. *Acc. Chem. Res.* **1968**, *1*, 136. (b) Cramer, R. *Ibid.* **1968**, *1*, 186. (c) Vaska, L. *Ibid.* **1968**, *1*, 335. (d) Heck, R. F. *Ibid.* **1969**, *2*, 10. (e) Parchall, G. W. *Ibid.* **1970**, *3*, 139. (f) Halpern, J. *Ibid.* **1970**, *3*, 386.
(3) Stille, J. K.; Lau, K. S. Y. *Acc. Chem. Res.* **1977**, *10*, 434.
(4) Trost, B. M. *Acc. Chem. Res.* **1980**, *13*, 385. Trost, B. M. *Tetrahedron* **1977**, *33*, 2615.
(5) Collman, J. P.; Cawse, J. N.; Kang, J. W. *Inorg. Chem.* **1969**, *8*, 2874.
(6) Heck, R. F. *Acc. Chem. Res.* **1979**, *12*, 146.
(7) Kochi, J. K. *Acc. Chem. Res.* **1974**, *7*, 351.
(8) Rappoport, Z. *Recl. Trav. Chim. Pays-Bas* **1985**, *104*, 309. Rappoport, Z. *Acc. Chem. Res.* **1981**, *14*, 7. Modena, G. *Ibid.* **1971**, *4*, 73.
(9) Stang, P. J.; Hanack, M.; Subramanian, L. A. *Synthesis* **1982**, 85.
(10) Stang, P. J.; Rappoport, Z.; Hanack, M.; Subramanian, L. R. *Vinyl Cations*; Academic: New York, 1979.

0002-7863/87/1509-1150$01.50/0